6 March 1970, Volume 167, Number 3923 **SCIENCE**

Preliminary Examination of Lunar Samples from Apollo 12

A physical, chemical, mineralogical, and biological analysis of 34 kilograms of lunar rocks and fines

The Lunar Sample Preliminary Examination Team (*1*)

This is the first scientific report on the examination of the samples returned from the Apollo 12 landing at a site south-southwest of Copernicus in Oceanus Procellarum on 19 November 1969. Most of these lunar samples have been in the Lunar Receiving Laboratory (LRL) at the Manned Spacecraft Center in Houston, Texas, since 25 November 1969, undergoing physical, chemical, mineralogical, and biological analysis.

The Ocean of Storms samples may be contrasted with those from Tranquillity Base in a number of ways: (i) While still old by terrestrial standards, the Apollo 12 rocks are about 1 billion years younger than those of Apollo 11. (ii) About half of the Apollo 11 material was microbreccia, as opposed to only 2 of the 45 rocks of Apollo 12. (iii) The regolith at the Apollo 12 site is about one-half as thick as at the Apollo 11 site. (iv) The amount of solar wind material in the Apollo 12 fines is considerably lower than in the Apollo 11 fines. (v) The crystalline rocks in the Apollo 12 collection display a wide range in both modal mineralogy and in primary textures, in contrast to the uniformity of the Apollo 11 rocks. (vi) The "nonearthly" chemical character of the Apollo 11 samples (high in refractory and low in volatile element concentrations) is shared by the Apollo 12 samples, but to a lesser degree. (vii) The chemical composition of the fine material is the same as that of the breccias but is different from that of the crystalline rocks; this is not as pronounced in the Apollo 11 collection.

Apollo 12 Mission

Four separate groups of samples (Table 1) were collected on the lunar surface during the two 4-hour periods of extra-vehicular activity (EVA). Other scientific tasks performed during EVA were photography of rocks, the lunar surface, and the moonscape; deployment of the Apollo Lunar Surface Experiments Package (ALSEP), which consisted of a central power station, a passive seismometer, a cold-cathode ion gauge, a suprathermal ion detector, a solar wind spectrometer and magnetometer; collection of pieces of Surveyor III; and deployment of the solar wind foil.

The functions of the preliminary examination, the procedures within the LRL, the reasons for the sample quarantine, and the tools used by the astronauts are all given in the Apollo 11 report (*2*).

Geologic Setting

The Intrepid landed on the northwest rim of the "Surveyor" crater (in which Surveyor III had landed on 20 April 1967) at 23.34°W and 2.45°S, about 120 km southeast of the crater Lansberg. The site is on a broad ray of Copernicus.

The landing site is characterized by a distinctive cluster of craters ranging in diameter from 50 to 400 m (Fig. 1). Informal names given to these craters for use during the mission have been adopted for this report. The traverses by the astronauts were generally on or near the rims of these craters and on deposits of ejecta from them.

The lunar surface at the landing site is composed of fragmental material, the regolith which ranges in size from particles too fine to see with the naked eye to blocks several meters across. Along many parts of the traverse made during the second period of EVA, the astronauts found fine-grained material of relatively high albedo. This material is at the surface in some places. It is possible that this discontinuous deposit of light gray material may be the feature that is observed telescopically as a ray of Copernicus. Darker regolith material that generally overlies the light gray material is only a few centimeters thick in some places, but probably thickens greatly on the rims of some craters. The size, shape, and relative abundances of the constituent particles and presence or absence of patterned ground vary from place to place. Most of the differences are probably the result of a small number of local cratering events.

Beads and irregularly shaped small fragments of glass are abundant both on and within the regolith; glass is splattered on some of the rocks at the surface and within many of the shallow craters.

The larger craters at the landing site are widely different in age as shown by large differences in the shapes of craters and the alteration of the ejected material. The age from oldest to youngest is interpreted as follows: (i) "Middle Crescent" ("1000 foot") crater, (ii) "Surveyor" and "Head" craters, (iii) "Bench" crater, (iv) "Sharp," "Halo," and "Block" craters.

At Middle Crescent crater the astronauts noticed large blocks on its wall that were probably derived from the

Table 1. Apollo 12 sample return. Fines are less than 1 cm, chips are between 1 and 4 cm. ALSRC, Apollo Lunar Sample Return Container.

Sample	Mass (g)	Container	Gas pressure in container on receipt at LRL
	Contingency sample		
Fines	1,102	Teflon bag	1 atm
Chips	9		
Rocks (4)	821		
	Selected sample		
Fines	2,716	1st ALSRC	2 to 4 × 10^{-4} torr
Chips	50		
Rocks (20)	11,940		
Core tube (19 cm)	101		
	Documented sample		
Fines plus chips	650	2nd ALSRC	0.5 atm
Rocks (6)	6,124		
Documented bags (13)			
Fines plus samples (7)	1,353		
Rock samples (11)	2,288		
Core tube			
(40 cm, double tube)	246		
(unopened)	80		
Lunar Environment Sample	269	LES container	?
Gas Analysis Sample	57	GAS container	?
	Tote bag sample		
Fines	21	Teflon bag	1 atm
Chips	10		
Rocks (4)	6,488		

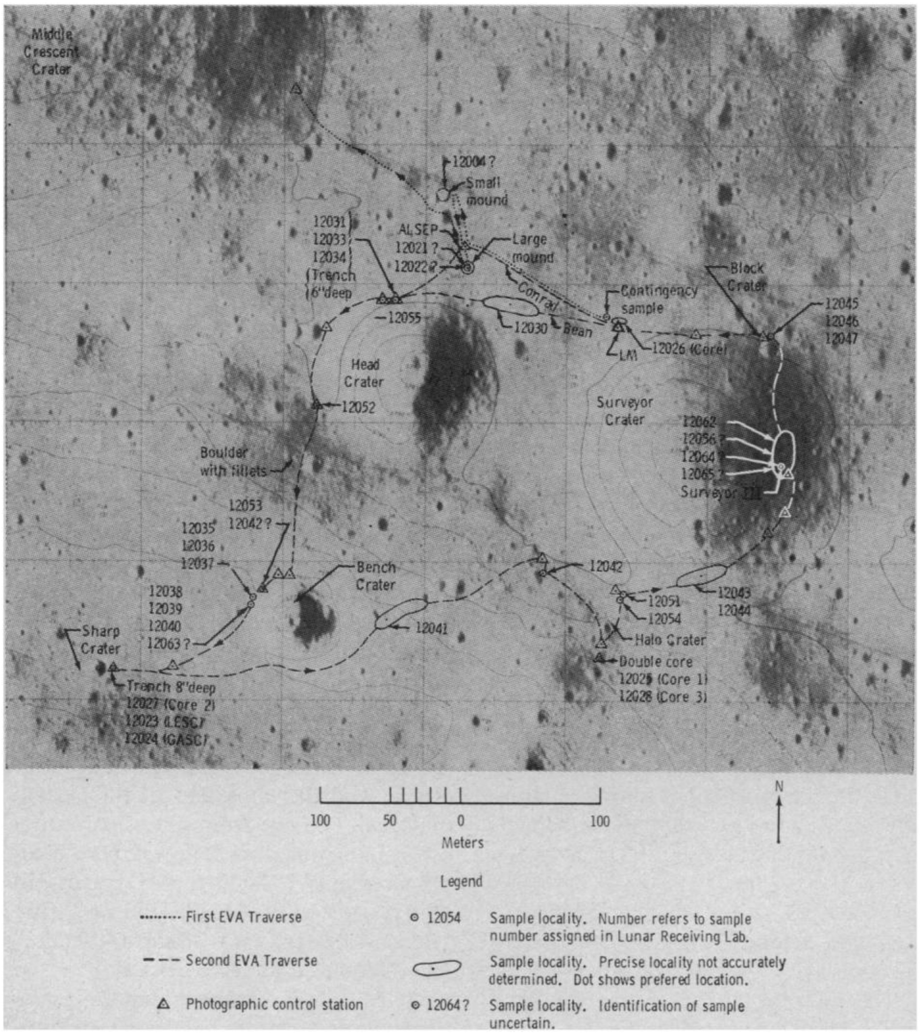

Fig. 1. Apollo 12 landing site.

local bedrock; large rock fragments in this crater probably have been exposed the longest and represent the deepest layers excavated by cratering at the site.

Rounded and angular blocks litter the surface of the rims of Head and Bench craters. Some rocks appeared coarse grained to the astronauts; their crystals were clearly visible. Many rocks on the rim of Bench crater appeared to be splattered with glass.

Three small, very fresh, blocky-rimmed craters apparently penetrate through the regolith into underlying materials. The craters are Sharp crater, about 14 m across and 3 m deep; Block crater, about 13 m across and 3 m deep; and a small crater 4 m across that lies on the south rim of the Surveyor crater just north of Halo crater. Samples were collected from these craters.

Sharp crater has a rim two-thirds of a meter high composed of material with high albedo. This material has been splashed out radially around the crater and is softer than the normal regolith. A core tube driven in the rim penetrated the ejecta without difficulty. Samples collected here may show the youngest exposure ages. The crater appears to have just penetrated the regolith; a terrace on its floor is probably controlled by bedrock.

At Block crater, high on the north wall of Surveyor crater, the ejected blocks are nearly all sharply angular, which suggests that it is very young. Many of the blocks show lines of vesicles similar in appearance to vesicular lavas on earth, the blocks probably are older, coarse, blocky, ejecta deposit underlying the rim of the Surveyor crater.

The 4-m blocky crater on the southern crest of the rim of Surveyor crater may have been excavated in an old rim deposit. Here the regolith is very thin.

The rocks collected from the Apollo 12 landing site are predominantly crystalline. At the Apollo 11 site about half the rocks collected were crystalline and half were microbreccia. The difference very likely is due to the fact that the Apollo 12 rocks were collected primarily on or near crater rims. On these rims the regolith is thin or weakly developed and many of the rocks are probably from craters that have been excavated in bedrock well below the regolith. Tranquillity Base, in contrast, is on a thick, mature regolith where many of the rock fragments were produced by induration of regolith material to form a breccia and were ejected from craters too shallow to excavate bedrock.

Lunar Soil Mechanics

The Apollo 12 regolith is, in general, similar to the regolith at Tranquillity Base. Similar penetrations of the Lunar Module (LM) footpads were observed under similar conditions, which indicated that the soil bearing capacities at the two sites are of the same order of magnitude. Bootprint depth was about the same at the two sites, less than 1 cm in the immediate vicinity of the LM and in the harder soil areas, and up to several centimeters in soft soil areas, especially in the rims of small and relatively young craters. Also similar are color, grain size, adhesion, and cohesion of most of the soil samples.

The two sites were significantly different in these respects. The Apollo 12 astronauts experienced greater loss of visibility due to soil erosion during the LM landing than did the Apollo 11 astronauts. This was due to different soil conditions or to a different descent profile (or both) at the two landing sites. The Apollo 12 astronauts were able to drive the core tubes to the full depth, approximately 70 cm for the double core tube, whereas the Apollo 11 astronauts were able to drive the tubes only about 15 cm. A different bit design probably helped in driving the tubes. The Apollo 12 trenches were dug to a depth of 20 cm, and the astronauts reported that they could have been dug considerably deeper without difficulty. The Apollo 11 astronauts could only dig down about 10 cm.

The ground surface has undergone little change in the past 2½ years, as judged by preliminary examination of the photographs taken by the astronauts at the Surveyor III site. The trenches excavated by the Soil Mechanics Surface Sampler of the Surveyor as well as the waffle pattern of the imprint of the surveyor footpad are much the same as when they were formed. The Surveyor was coated with a thin layer of dust.

Mineralogy and Petrology

The majority of the large rock samples returned by Apollo 12 are holocrystalline, with a range of textures and mineralogical compositions that are characteristic of igneous origin. Two breccias were also returned. The crystalline rocks are similar to the microgabbros and basaltic rocks from Apollo 11 in that they consist essentially of clinopyroxene, calcic plagioclase, olivine, and ilmenite. However, they differ in that they exhibit a wide range of modal mineralogy, grain, size, and texture.

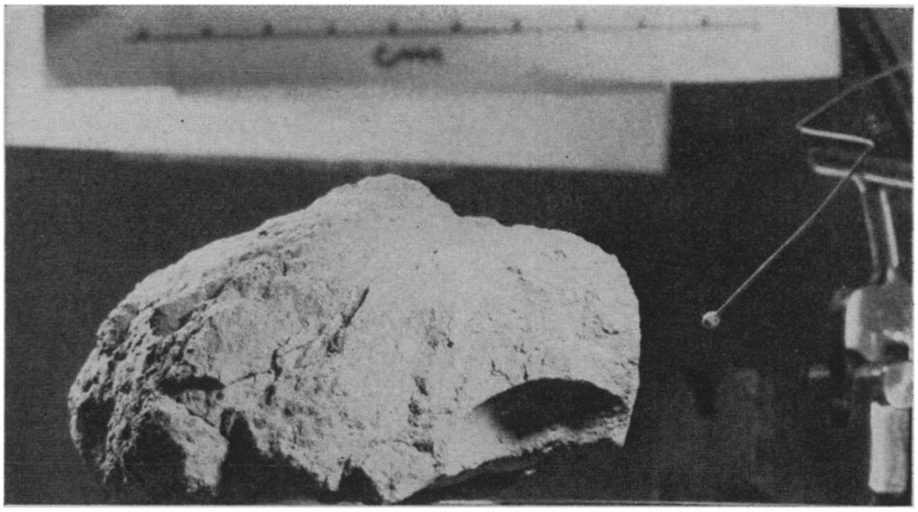

Fig. 2. Sample 12009. This rock, along with sample 12015, displays several large (up to 8 cm) egg-shaped, smooth-walled vesicles. The walls of these vesicles consist of a matte of plagioclase and pyroxene crystals. Rock 12015 is highly shocked, containing about 80 percent glass. NASA photo S-69-62300.

Igneous Rocks

About one-half of the igneous rocks have vesicles present, and all have vugs. The vesicles range in diameter from 0.1 mm to 40 mm (Fig. 2) and are commonly lined by crystals of plagioclase, pyroxene, or olivine oriented tangential or subparallel to the walls. The vugs contain euhedral crystals of pyroxene and olivine (Fig. 3), and less well formed crystals of plagioclase, ilmenite, and spinel. The volume occupied by vugs and vesicles in any rock is generally less than those from Tranquillity Base. The vugs are irregular and in the coarser rocks occur at the termination of sheaf-like aggregates of pyroxene and plagioclase. In one sample pyroxene crystals appear in raised relief along a joint surface. Crystals in vugs and along

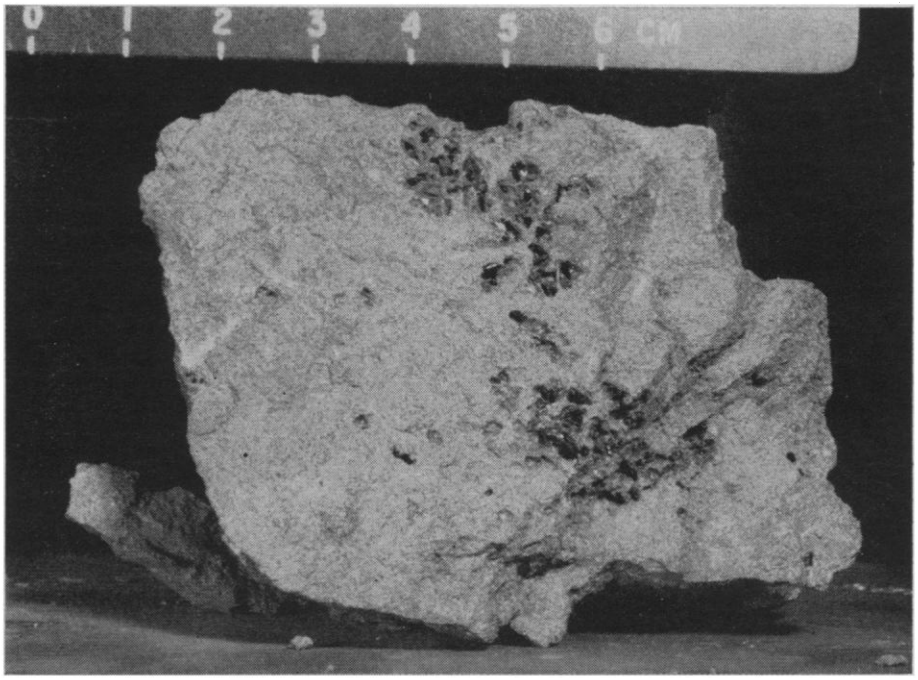

Fig. 3. Sample 12052, a typical equigranular crystalline rock. Note the concentration of vugs, perhaps forming a stratigraphic layer. Vugs contain large euhedral crystals of pyroxene and olivine. NASA photo S-70-21320.

joints are considerably coarser than the groundmass minerals. Variations in cooling rates can explain the variety of grain sizes observed.

The grain size of the igneous rocks ranges from 0.05 mm to 35 mm. The textures show remarkable variations (Fig. 4), many of which are common to volcanic and plutonic rocks on earth. Many of the rocks are equigranular gabbros, some are ophitic and subophitic diabases, and others are variolitic basalts. Feathering sheaves of pyroxene-plagioclase intergrowths are found in the groundmass of porphyritic rocks that contain phenocrysts of pigeonite. The olivine crystals in most rocks are equant euhedral grains somewhat coarser than the groundmass.

The mineralogical composition of the rocks reflects the high iron content. The lower titanium contents compared to the Tranquillity Base rocks are reflected in the smaller amounts of ilmenite. The textural and mineralogical variations can be explained readily by fractional crystallization and mineral accumulation during the cooling of basaltic magmas.

The modal mineralogy shows a wide variation (Fig. 5), especially as contrasted with the Apollo 11 modes. The modes range from pyroxene-rich peridotites (12075: pyroxene 50 percent, olivine 40 percent, plagioclase 10 percent), olivine gabbros (12036: pyroxene 25 percent, olivine 40 percent, plagioclase 25 percent, ilmenite 10 percent), and gabbros (like the Apollo 11 rocks) to troctolites (12035: pyroxene 15 percent, olivine 40 percent, plagioclase 45 percent).

Rock 12013 consists largely of plagioclase and sanidine, and appears to be a late-stage differentiate on the basis of its modal mineralogy and trace element content.

Some rocks show evidence of planar features, such as fractures and lines of vugs, but generally the rocks are without marked foliation or lineation. All of the rocks are fresh and show no evidence of the hydration or oxidation reactions common during late-stage terrestrial magmatic processes.

Mineralogy

Minerals identified in the Apollo 12 samples are similar to those observed in the Apollo 11 materials. Glass, plagioclase, pyroxene, olivine, low cristobalite, ilmenite, sanidine, troilite, and iron metal have been positively identified. Spinel, tridymite, metallic copper, and the iron analog of pyroxmangite were tentatively identified by optical methods.

Plagioclase is present in every rock sample, from about 5 to 10 percent (12075) to 70 percent (12013). Estimates of composition based on extinction angle measurements and indices of refraction range from An_{50} to An_{90} (50 to 90 mole percent anorthite, $CaAl_2Si_2O_8$) with the median value falling near An_{80}. Some plagioclase is zoned, most is twinned, and lath-shaped crystals prevail.

Pyroxenes, the dominant minerals in most samples, were identified by x-ray diffraction and by optical properties.

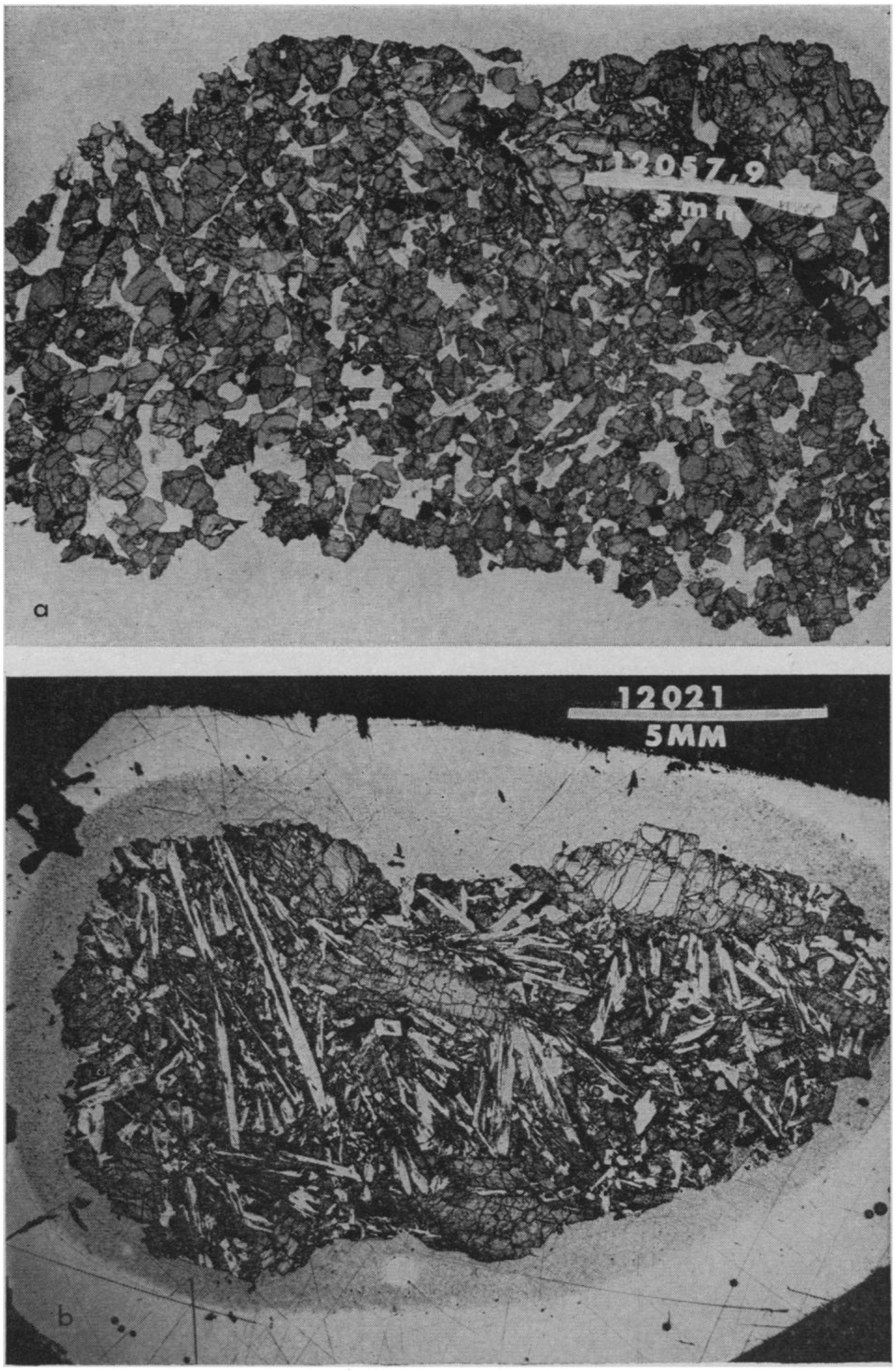

Fig. 4. Thin sections illustrating the various textures displayed by the Apollo 12 crystalline rocks. (a) Olivine basalt from a chip of smple 12057. NASA photo S-69-63409. (b) Porphyritic gabbro with variolitic texture. Phenocrysts are pigeonite. Radiating laths are an intergrowth of pyroxene and plagioclase. Sample 12021; NASA photo S-70-20749. (c) Sample 12065 illustrating a mafic rock. The texture is variolitic. Plagioclase is about 15 percent in this sample. The lath-shaped crystals are pyroxene; the equant crystals are olivine. NASA photo S-69-63405. (d) Sample 12022 illustrating an equant texture in a mafic rock. The large equant crystals are olivine. NASA photo S-70-20740.

Pigeonite and subcalcic augite are the most common, as determined optically. Refractive indices indicate that Fe/(Fe+Mg) is about 0.5. Zoned pigeonite phenocrysts occur in porphyritic and coarse-grained rocks. Pigeonite occupies the cores of some crystals, and subcalcic augite of deeper brown color than the pigeonite forms the rim. The groundmass pyroxenes are fine grained, darker in color than phenocrysts, and are not zoned. Intergrowths of pyroxene and plagioclase are common and range in size from crystals that are 1 cm long to aggregates whose individuals are only several micrometers across.

Olivine occurs in nearly all samples, in contrast with the Apollo 11 samples, and was identified by x-ray diffraction and by optical properties. Estimates of composition based on optical properties disagree with those based on x-ray data. The discrepancy is due to a fairly high calcium content as indicated by spectrography. The samples for which x-ray, optical, and spectrographic analyses are available indicate a composition of about $(Ca_{.05}Mg_{.60}Fe_{.35})_2SiO_4$. Olivine commonly contains inclusions of devitrified glass or aggregates of plagioclase, pyroxene, and ilmenite. Some grains contain spherical glass inclusions. Grains of fayalite, the iron end member of the olivine group, were tentatively identified by their optical properties. Sanidine was tentatively identified by x-ray diffraction and optically identified in the thin section of sample 12013. Low cristobalite occurs as interstitial aggregates and euhedral to subhedral crystals. Ilmenite, identified by x-ray diffraction, morphology, and optical properties, ranges in abundance from less than 1 percent to 25 percent. In reflected light some grains showed intergrowths with another unidentified oxide. The presence of spinel is suggested by the octahedral forms of opaque minerals of unknown composition which occur within olivine grains and in vugs. At least three other unidentified opaque phases are also present. Troilite is ubiquitous in all polished thin sections. Metallic iron occurs as interstitial blobs commonly not associated with troilite grains, rather than as blobs in troilite as noted in Apollo 11 samples. It is more commonly associated with ilmenite than with any other mineral. Glass occurs as minute interstitial material in some crystalline rocks, and as beads and groundmass in clastic rocks and as a thin coating on several rocks.

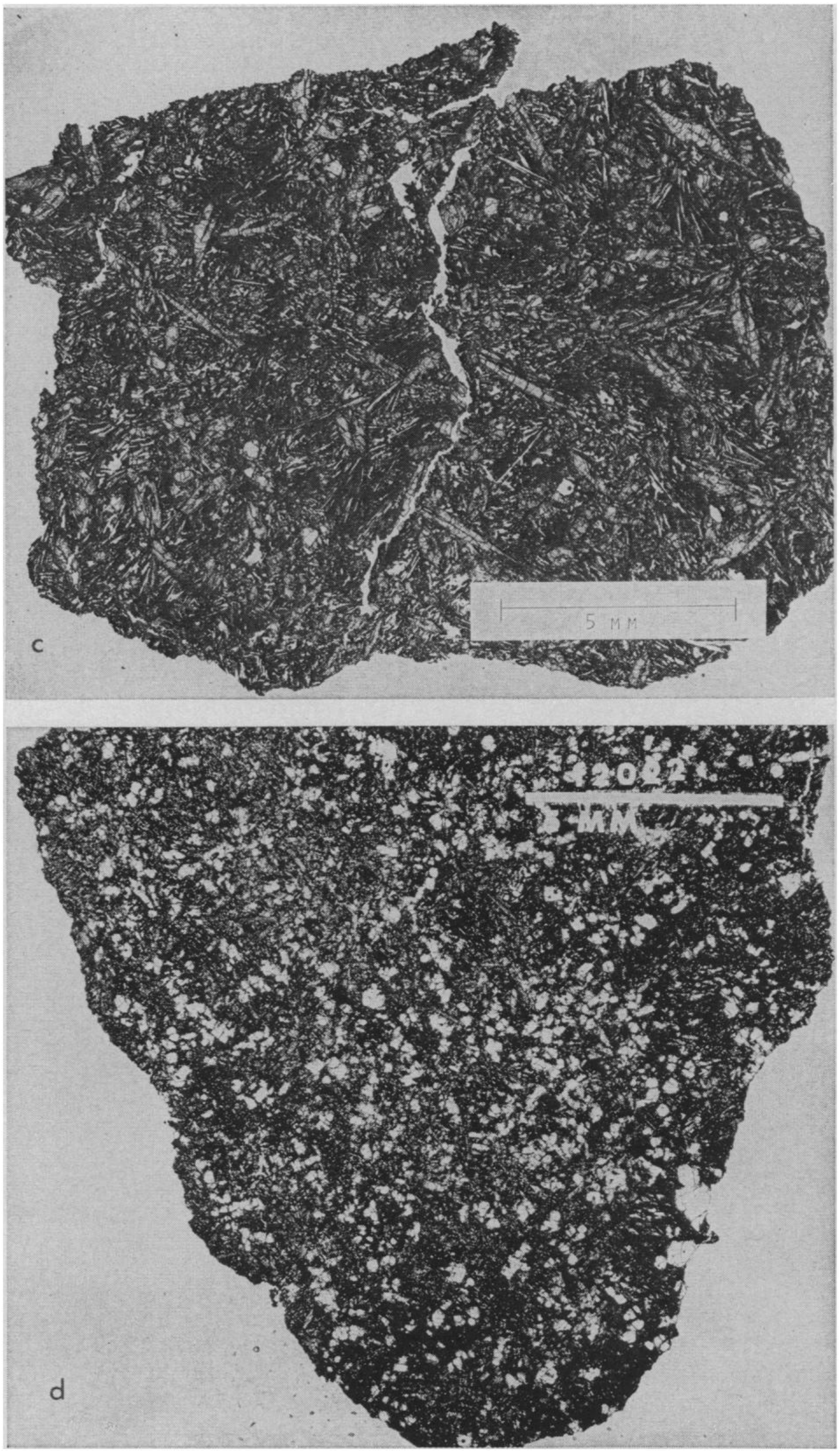

Breccias

One rock is a fragmental breccia similar to the Tranquillity Base breccias. Two breccia chips were also collected. The dominant constituents of the breccias appear to be pyroxene and plagioclase with accessory olivine and glass; lithic fragments are also present (Fig. 6). The average mineral composition is less olivine-rich than that of the majority of rocks collected. The rock appears to have a foliation developed in which both lithic and mineral fragments are subparallel. The lithic fragments are as large as 20 mm by 10 mm and are both igneous and fragmental rocks, indicating more than one period of fragmentation and consolidation.

Rock Surface Features

Most of the larger Apollo 12 crystalline rocks are similar to the Apollo 11 rocks in that they are rounded on one surface and exhibit glass-lined pits. Other surfaces may be angular and fractured. Small pits occur on rock surfaces, with a density that ranges from 1 to 30 per cm^2; angular bottom surfaces have few or no pits. Pits visible under a binocular microscope are 0.1 mm to 1 cm in diameter with a depth-to-width ratio of approximately 1 to 5. Most of the pits are circular, but a few are oval, with the long axis parallel to elongate feldspar or pyroxene crystals in coarse crystalline rocks. Glass lining the pits varies greatly in thickness and vesicularity. Pulverized minerals form white halos, 0.5 to 1.0 crater-widths wide, around pits on crystalline rock surfaces. Where pit density is high, a crust 1 to 2 mm thick of pulverized minerals is formed on the rock surface. Impact pits in glass coatings are surrounded by radiating fractures. On many of the medium- to coarse-grained crystalline rocks, the glass pit linings are raised slightly above the rock surface. These glass-topped pedestals appear to be more resistant to erosion than the rock.

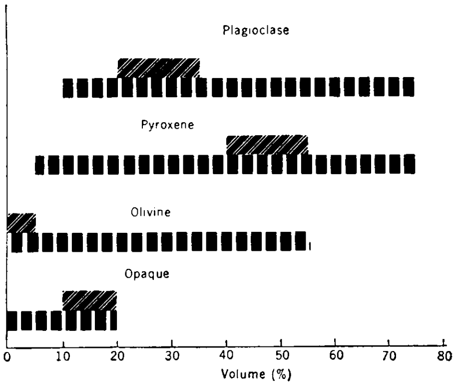

Fig. 5. Comparison of range of modal mineralogy of Apollo 11 (diagonal) and Apollo 12 (vertical) rocks.

Irregular patches of glass have been spattered on rock surfaces. Two types which grade into one another can be distinguished—thin films (less than 0.1 mm thick) and thick (0.1 to 1 cm), highly vesicular coatings. The thin films are brownish-black in reflected light and brown in transmitted light, cover 1 to 16 cm^2, are usually slightly vesicular, and adhere tightly to the rock surface. The thick layers found on samples from the bottom of a 1-m crater are light to dark brown, have vesicles that increase in size from 0.1 mm to several millimeters from the base to the outer surface, and have smooth botryoidal surfaces (Fig. 7). These thick films coat several highly fractured breccias and fine-grained crystalline rocks, filling fractures in the rocks to a depth of several centimeters. Contacts between glass and rock are sharp. Some glass coatings contain many angular, highly shocked rock chips. Some of the vesicular glass has been partly devitrified. A light gray glass of uncertain origin with pronounced flow structure was also collected.

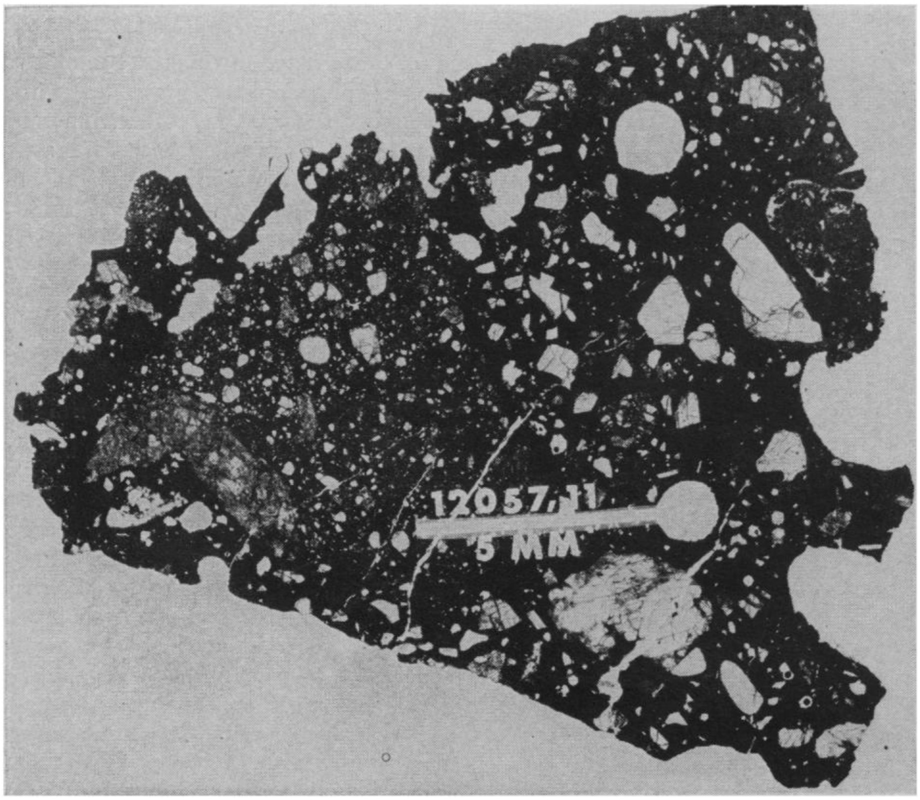

Fig. 6. Thin section of a chip of sample 12057 (a breccia). Note spherules in matrix. NASA photo S-69-63407.

Fines

The Apollo 12 fines contrast with the Apollo 11 fines in that they consist of different proportions of phases and are lighter in color. The major constituents in decreasing order of abundances are pyroxene, plagioclase, glass, and olivine. The minor constituents, totalling only a few percent, are ilmenite, tridymite, cristobalite, nickel-iron, and several unidentified phases. The iron analog of pyroxmangite was tentatively identified.

Glass totals roughly 20 percent in the Apollo 12 fines. It includes spheroidal and dumbbell-shaped objects and angular fragments. The glass ranges from colorless through pale yellow brown and brown to dark brown; the index of refraction generally is in the range from 1.55 to 1.75. Bubbles and solid inclusions are common in the colored glasses. In contrast to the Apollo 11 fines, feldspar glass, dark-colored to nearly opaque spheroidal glass, and fragments of dark scoriaceous glass are relatively rare.

The pyroxenes, mostly pale yellow to tan and brown in color, range widely in composition and include augite, subcalcic augite, and pigeonite. They constitute about 40 percent of the whole. The range of indices of refraction are somewhat greater than those of the pyroxenes of the Apollo 11 fines. Plagioclase has indices of refraction mostly in the range of the more calcic members, bytownite and anorthite. A small amount of more sodic plagioclase is also present. The olivine totals about 5 to 10 percent and is more abundant than in the Apollo 11 fines. The few measured grains fell in the compositional range Fo_{60} to Fo_{70} (60 to 70 mole percent forsterite, Mg_2SiO_4). Many lithic fragments are present. Low tridymite is in the form of anhedral grains, and low cristobalite occurs as microgranular aggregates.

There are two light gray fines samples of notably different character—one consists of the light layers in the double core tube, and the other is sample 12033, a documented sample taken in a trench dug near the northwest rim of Head

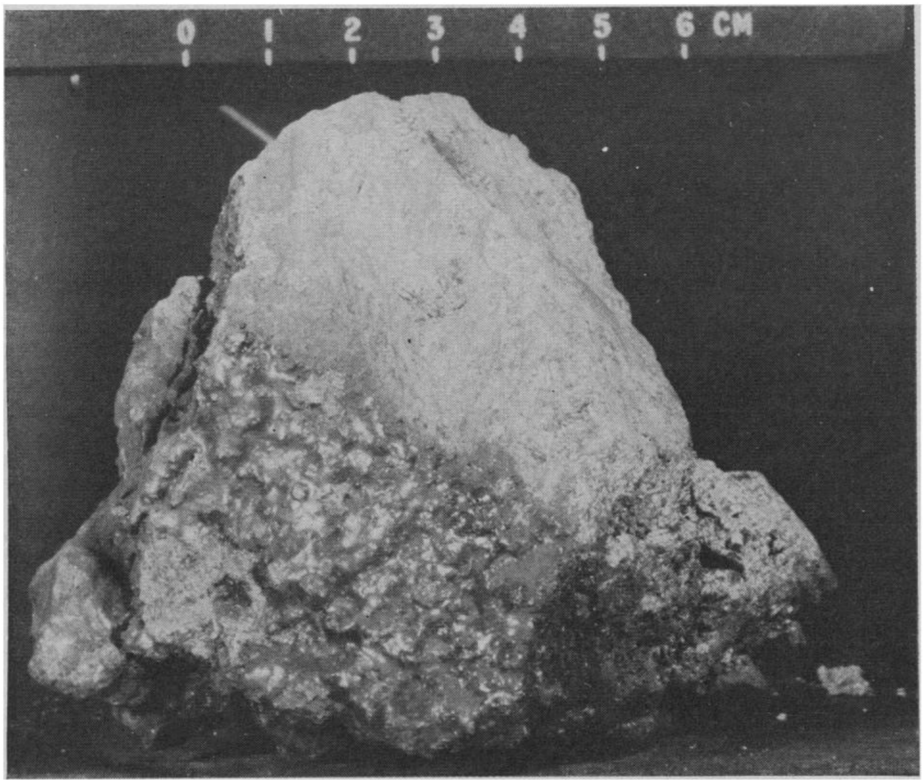

Fig. 7. View of sample 12054. This photo illustrates a 1-mm thick black glass coating that is sealing a fracture (on the left-hand side). The part of the sample that is not glass-coated is striated. NASA photo S-69-60972.

crater. Sample 12033 consists of clear angular grains of feldspar with some olivine, pyroxene, and abundant basaltic glass. The coarser (1-mm diameter) glass fragments are pumiceous and exhibit well-developed flow structure and stretched vesicles; finer fragments are angular and somewhat vesicular. The finer shards also contain flow structure, consisting of oriented microlites. This sample is tentatively considered to be crystal-vitric ash, with many of the characteristics of terrestrial volcanic ash.

The fines contain many very well rounded grains, with minutely chipped surfaces, that resemble grains in terrestrial detrital sands. Many are slightly elongate, oblate bodies with a bean-like shape. They range in size down to well below 0.1 mm. Presumably the result of mechanical abrasion, they are chiefly glass, but some are pyroxene, plagioclase, or intergrowths of these minerals.

Impact Metamorphism

Impact metamorphism in Apollo 12 samples is similar to and as common as in the Apollo 11 samples. Impact-fused glass spherules and beads and shock-vitrified mineral fragments are present both in the fines and in the microbreccias. Most of the large Apollo 12 crystalline rocks are apparently unshocked or only weakly shocked, but several crystalline rocks show moderate to strong shock. A thin section of one of these showed extensive fracturing of the plagioclase and partial vitrification and development of lamellar microstructures. The coexisting clinopyroxenes show one to two sets of closely spaced lamellar twinning that are absent in clinopyroxene of similar unshocked crystalline rocks. Another sample shows extensive shock vitrification.

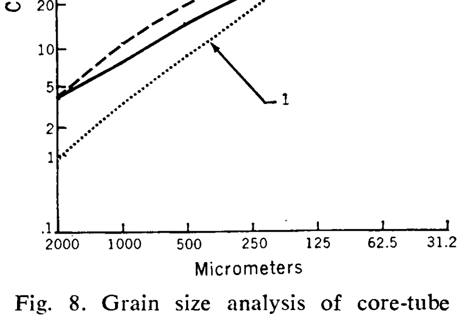

Fig. 8. Grain size analysis of core-tube material; 1, 2, and 3 are top, middle, and bottom of tube 12026; 4 is the coarse layer in tube 12028.

Shocked microbreccia is also present. Many small fractured microbreccia fragments are held together by glass spatters. Also present is breccia within breccia indicating a history of multiple shock.

Small pebbles were collected which are either glassy or aphanitic, and are highly vesicular or vuggy. They are presumably the result of melting and fragmentation as a result of impact metamorphism. Some of the vesicles are as large as 10 mm in diameter and occupy up to 50 percent of the preserved fragment.

Drive-Tube Core Samples

The core samples differ from those collected at Mare Tranquillitatis in having easily recognizable stratigraphy and two coherent crust-like layers, but otherwise they resemble the earlier cores in the dominantly fine-grained textures and loose consistency; in the restricted range of medium gray colors and fresh, unoxidized appearance; and in the abundance of glass, including some spherules. Dissection of these cores produced weakly coherent ephemeral structures ranging from fine subrounded crumb-like units 1 to 2 mm in diameter to subangular blocky or occasional angular units with maximum dimensions of 5 mm. Coherence was adequate to permit dissection with care of small vertical faces 1 cm high before slumping occurred.

All cores opened were broken by fine fracture planes, usually transverse to the core tube. Where such fractures coincide with changes in character of the sediment, they are interpreted as bedding planes. Other more complex fracture zones not coinciding with morphologic changes may be shear fractures produced when the drive tubes were rotated as the samples were collected.

The core collected on the first EVA is 19.3 cm long, and is uniformly medium to dark gray. Stratification shows clearly in the abrupt change in abundance of rock fragments and glass particles coarser than 1 mm below a transverse fracture at a depth of 5.9 cm. This stratification is reflected also by changes in mean grain size with depth (Fig. 8). Due to coherence of fine particles it was not possible to obtain reliable

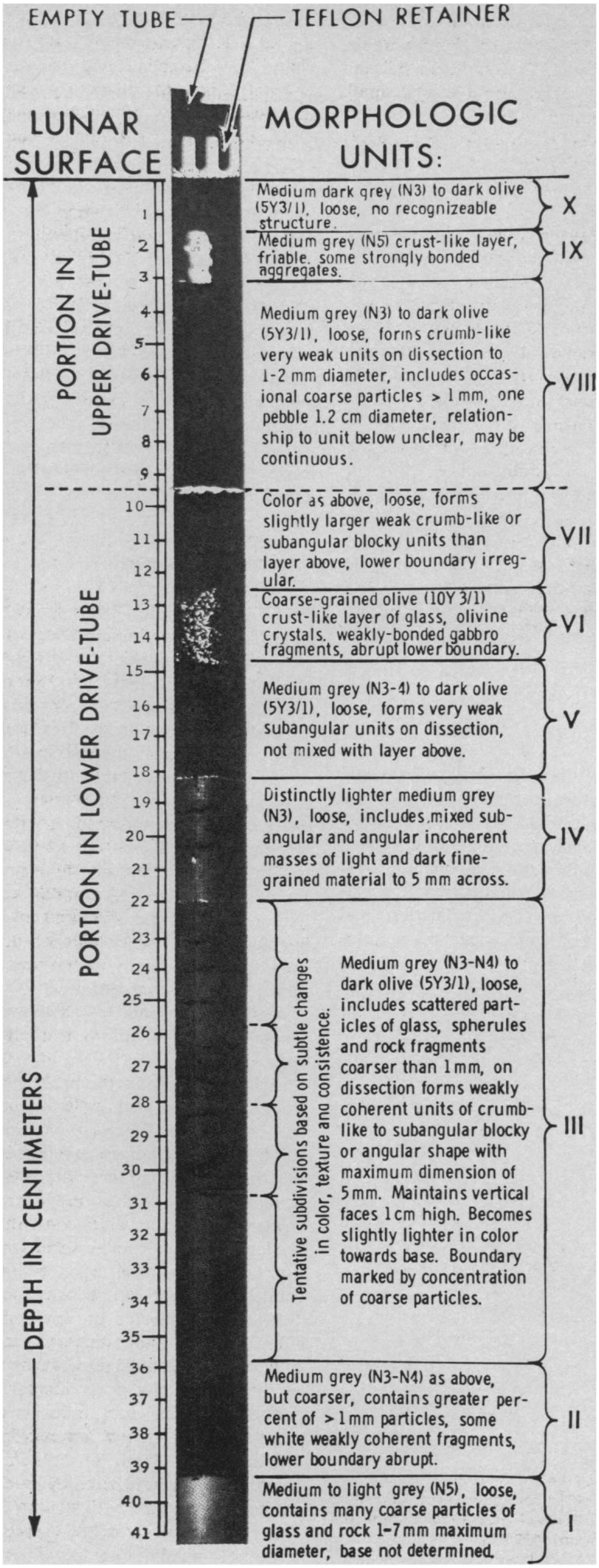

Fig. 9 (left). Schematic diagram of the double core tube which describes the layering present.

mechanical analyses below 0.062 to 0.031 mm. Material coarser than 2.00 mm could not be analyzed due to the limited sample size.

The three mechanical analyses taken from the first core are similar to those made of Apollo 11 cores. The slope of the cumulative curves, and hence the sorting, is very similar for all three samples. However, deeper samples are progressively coarser. The median grain size changes from 0.062 mm in the surface sample to 0.074 mm in the middle sample to 0.11 mm in the deepest sample.

Stratification and morphological change are most evident in the core collected in the double tube used at Halo crater (Fig. 9). The entire lower tube (32 cm) and 9.3 cm of the upper tube were filled with sediment. At least ten layers or horizons have been recognized. The most distinctive of these units is a coarse layer of angular rock fragments, minerals, and glass, comprised mostly of olivine grains and olivine-rich gabbros. The fourth mechanical analysis is of this coarse layer. The slope of the cumulative grain size curve, and therefore the sorting, is similar to the fine material but displaced markedly toward the coarse end of the graph. Extrapolating to the 50th percentile, the median grain size is approximately 4.9 mm.

The sharp contact with the fine material above and below the coarse layer, as well as its lack of fines, suggests that it is of primary impact origin. The gradual increase in grain size with depth shown by the three analyses from the first core suggests also that grain size of the debris has decreased due to reworking.

Other units found in the deep core include a fine-textured zone of lighter medium gray material, a zone of mixed incoherent light and medium gray sediments, and at the base of the core a layer of much lighter gray material. This lowermost layer is similar in appearance to sample 12033.

Both the coarse layer and a medium gray layer 2 cm thick, just below the surface at the Halo crater site, have a friable consistency unlike any core materials observed previously, and particles coarser than 1 mm in both layers may be strongly bonded aggregates indigenous to the layers rather than admixed fragments.

Chemistry

Chemical analyses of the samples were carried out mainly by optical spectrographic techniques conducted inside the biological barrier. A Jarrell-Ash Ebert instrument with a dispersion of 5.2 Å/mm was used.

The major constituents of the samples are, in general order of decreasing abundance, Si, Fe, Mg, Ca, Al, and Ti. The major silicate and oxide mineral phases present in the samples allow the deduction that oxygen comprises the major anion. Chromium, Na, Mn, and K are minor constituents, with concentrations ranging from 0.05 to 0.06 percent. Occasionally Ba and Zr reach these concentrations. The other constituents are present mostly at less than 200 parts per million (0.02 percent). The volatile elements (Pb, B, Bi, Tl, and so forth) are generally below the limits of detection of the spectrographic methods employed, although Pb ($\sim$30 ppm) and B ($\sim$20 ppm) were detected in sample 12013. Gold, silver, and the platinum group elements were not detected in any samples.

The chemistry of the crystalline rocks are lower in Rb, K, Ba, Y, Zr, and Li and higher in Fe and Cr. Several critical element ratios are likewise distinct. The K/Rb ratios average 850 in the rocks compared to 450 in the fines. The Fe/Ni ratio in the rocks (average 3,000; range 2,000 to 11,000) is much higher than the ratio of about 600 in the fines. The Rb/Sr ratios, very low in the rocks (0.005), are higher (0.02) in the fines.

The fine material and the breccias are generally quite similar in composition, and could not have formed directly from the large crystalline rock samples. The nickel content of the breccias and fine material places an upper limit on the amount of meteoritic material contributed to the lunar surface regolith. Using an average meteoritic nickel content of 1.5 percent, the Ni content of the fine material represents a meteoritic contribution of the order of 1 percent if all the nickel were extralunar.

The crystalline rocks show minor but significant internal variation in chemistry (Table 2). They are tabulated in order of decreasing magnesium content, which appears to be the most significant parameter among the major constituents. A number of interesting geochemical trends appear when the samples are so arranged (Fig. 10). Nickel shows a striking decrease in concentration, by an order of magnitude. Chromium shows a smaller relative decrease in the same direction and cobalt shows a slight decrease. Silicon increases as Mg decreases. Similar trends are shown by V, Sc, Zr, Y, K, Ba, and Ca, although the variations are small. Critical elemental ratios Fe/Ni, Ni/Co, and Cr/V decrease and V/Ni increases with decreasing Mg. No significant trends are shown by K/Rb, Rb/Sr, or K/Ba ratios.

Rock 12013 is unique among lunar samples. It contains the highest concentration of SiO_2 (61 percent) yet observed and the amounts of K, Rb, Ba, Zr, Y, the rare earth element Yb, and Li are enriched by 10 to 50 times compared to the other rocks. These high concentrations are reminiscent of the terrestrial enrichment of elements in residual melts during the operation of fractional crystallization processes. Molybdenum, Fe, Cr, Mn, Ni, Ti, Sc, and Co are low in comparison with the other rocks, but are not strikingly depleted. Nickel, in particular, is not depleted, as it would be in terrestrial analogs. Sample 12033 from the light gray fine material shows some analogies in composition to the rock, containing high Yb, Nb, and Rb.

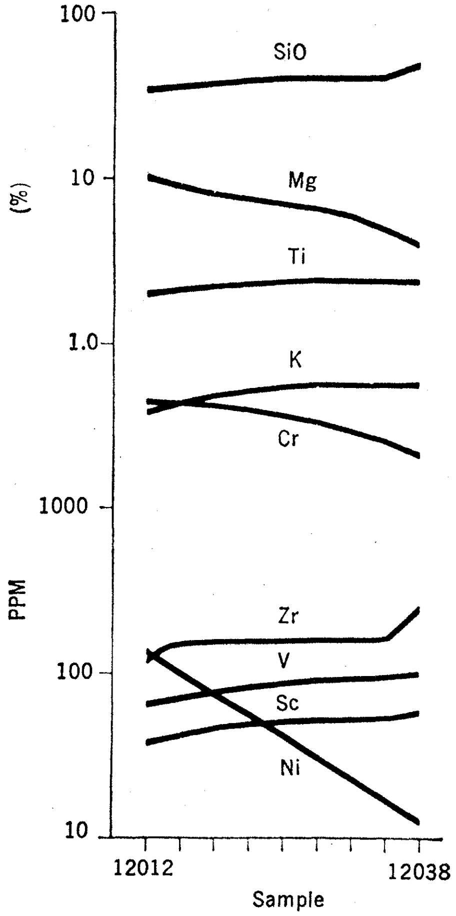

Fig. 10. Elemental variation within the crystalline rocks. Samples are arranged in order of decreasing Mg content. Note the decrease in Ni content by an order of magnitude in this sequence.

The chemistry at the two mare landing sites is clearly related. Both suites show the distinctive features of high concentrations of refractory elements and low contents of volatile elements which most clearly distinguish lunar material from other materials. In detail, there are numerous and interesting differences between the Apollo 12 and Apollo 11 rocks. These include:

1) Lower concentration of Ti, both in the rocks and the fine material of Apollo 12. The range in composition is 0.72 to 3.4 percent Ti (1.2 to 5.1 percent TiO_2) compared with the range in the Apollo 11 rocks of 4.7 to 7.5 percent Ti (7 to 12 percent TiO_2).

2) Lower concentrations of K, Rb, Zr, Y, Li, and Ba in Apollo 12 rocks.

3) Higher concentrations of Fe, Mg, Ni, Co, V, and Sc in the crystalline rocks from Apollo 12. These data are consistent with the more mafic character of the Apollo 12 rocks.

4) The significant variation in the Apollo 12 rocks is among the elements which favor ferromagnesian minerals. The range of abundance was not nearly as great in the Apollo 11 rocks.

5) The fine material at the Apollo 12 site differs from that at the Apollo 11 site in containing about half the titanium content, more Mg, and possibly higher amounts of Ba, K, Rb, Zr, and Li. The light gray fine material (12033) is strongly enriched in Rb, Zr, Yb, and Nb relative to the other fine material.

The chemistry of the Apollo 12 samples does not resemble that of chondrites, nickel in particular being strikingly depleted. The eucrite class of the basaltic achondrites are closest in composition, and sample 12038 shows some similarities in composition (Table 2). The felsic rock (12013) does not resemble terrestrial diorites, dacites, anorthosites, or tektites in the abundances of most elements.

The procedures were generally similar to those used to analyze the Apollo 11 samples, but modifications were made to cope more effectively with the high concentration of the refractory elements. For example, the ratio of admixed carbon to sample was increased from 1:1 to 4:1 for the method using Pd as an internal standard, and the range of intensity measurements possible was increased by a factor of 3, enabling a wider spread in concentrations to be effectively covered (for example, Ba and Zr).

The overall precision of the determinations is ± 5 to 10 percent of the amount present. Accuracy was controlled by use of the international rock

Table 2. Elemental abundances, expressed as parts per million except as noted for calcium, sodium, titanium, iron, magnesium, aluminum, and silicon. Also elemental abundances expressed as weight percent oxides. Sample 12013 also contains Pb, 30 ppm; B, 15 ppm; Nb, 170 ppm; and Yb, 20 ppm. Sample 12033 also contains Nb, 44 ppm; and Yb, 12 ppm.

	Crystalline rocks									Crystalline rocks average	Fines 12070	Breccia 12073	Breccia (?) 12010	Light-colored fines 12033	12013
	12012	12004	12015	12022	12009	12065	12052	12064	12038						
Rb	.64	.47	1.0	.17	.57	.72	.80	.76	.70	.64	3.2	4.9	2.0	7.5	33
Ba	38	60	44	38	65	70	50	55	230	72	420	510	180	720	2,150
K	460	480	510	560	520	600	570	700	470	540	1,500	2,100	1,300	3,240	1.66 (%)
Sr	110	145	115	160	110	135	135	165	230	145	170	230	145	260	150
Ca (%)	6.6	7.1	7.0	7.9	7.1	9.0	7.9	8.6	7.9	7.6	7.1	8.2	7.0	8.2	4.5
Na (%)	.39	.36	.27	.27	.38	.29	.33	.31	.45	.33	.30	.29	.39	.40	.51
Y	40	52	46	62	48	48	42	55	68	51	130	180	87	260	240
Zr	120	170	160	160	150	180	170	170	260	170	670	1,200	380	950	2,200
Cr	3,900	5,800	3,900	2,650	5,200	3,500	3,700	3,000	2,200	3,750	2,800	2,800	3,050	2,100	1,050
V	65	85	95	65	77	135	105	100	70	88	64	50	92	37	13
Sc	38	45	44	52	42	60	52	60	55	50	47	42	50	33	21
Ti (%)	1.9	2.0	1.9	3.4	2.0	2.3	2.2	2.9	1.9	2.3	1.9	1.9	2.2	1.6	.72
Ni	135	90	70	40	67	25	32	15	14	54	200	350	80	140	105
Co	48	50	47	36	46	34	42	40	23	40	42	30	39	34	13
Fe (%)	17.9	17.9	17.1	17.1	15.5	17.1	16.3	17.0	13.2	16.6	13.2	13.0	15.2	12.4	7.8
Mn	1,300	1,750	2,550	1,350	1,450	3,200	2,400	2,500	2,000	2,050	1,900	1,500	1,400	1,800	950
Mg	10.6	9.0	8.4	7.8	7.5	6.6	6.0	4.8	3.9	7.2	7.2	6.6	6.6	6.5	3.6
Li	3.9	4.2	10	3.1	5.5	6.0	4.5	6.7	5.5	5.5	11	25	7	15	100
Al (%)	5.7	5.6	5.8	5.8	5.7	6.4	5.8	6.3	6.4	5.9	7.4	7.9	6.1	8.5	6.3
Si (%)	16.4	17.3	17.8	16.8	19.2	18.2	19.6	18.7	22.9	18.5	19.6	19.1	20	19.2	28.5
SiO_2	35	37	38	36	41	39	42	40	49	40	42	41	43	41	61
TiO_2	3.1	3.4	3.2	5.1	3.3	3.8	3.6	4.9	3.2	3.7	3.1	3.1	3.7	2.6	1.2
Al_2O_3	11	10.5	11	11	11	12	11	12	12	11.2	14	15	11.5	16	12
FeO	23	23	22	22	20	22	21	22	17	21.3	17	17	19.5	16	10
MgO	17.5	15	14	13	12.5	9	10	8	6.5	11.7	12	11	11	11	6.0
CaO	9.3	10	9.8	11	10	12.6	11	12	11	10.7	10	11.5	10	11.5	6.3
Na_2O	.53	.48	.37	.36	.51	.39	.45	.42	.60	.45	.40	.50	.53	.54	.69
K_2O	.055	.058	.062	.068	.063	.072	.069	.084	.057	.065	.18	.25	.16	.39	2.0
MnO	.17	.23	.33	.17	.19	.41	.31	.32	.26	.26	.25	.19	.18	.23	.12
Cr_2O_3	.57	.85	.57	.39	.76	.51	.54	.44	.32	.55	.41	.41	.45	.31	.15
ZrO_2	.016	.023	.022	.022	.020	.024	.023	.23	.035	.023	.09	.16	.05	.13	.30
NiO	.017	.011									.025	.044		.018	.013
Total	100.2	101.1	99.4	99.6	99.1	99.8	100.0	100.2	100.0	99.9	99.5	100.2	100.1	99.7	99.8

Table 3. Abundances of noble gases in Apollo 12 lunar samples. Values are expressed as 10^{-8} ccSTP/g.

Sample	He	4/3	^{20}Ne	20/22	22/21	^{40}Ar	40/36	36/38	^{84}Kr	^{132}Xe
Fines										
12070	6,700,000	2,300	120,000	13.3	28	12,000	0.60	5.1	13	2.6
12060	4,000,000	2,100	73,000	13.2	26	9,800	0.80	5.2	4	1.1
Breccia										
12034	130,000	940	8,700	12.0	13	3,500	2.1	4.8	0.95	1.1
12071	1,700,000	2,100	33,000	12.3	21	5,300	0.90	5.1	4.8	1.2
Typical crystalline rocks										
12062	9,000	59	63	2.4	1.3	1,400	57	0.98	0.07	0.021
12064	13,000	64	60	1.6	1.2	1,300	50	0.83	0.033	0.012
12004	15,000	200	46	3.6	1.5	900	97	1.9	0.02	0.014
Special cases										
12013	360,000	10,000	100	7.8	2.5	820,000	51,000	2.5	0.21	0.15
12010 (light)	24,000	270	20	5.2	1.8	1,400	72	1.6	0.015	0.017
12010 (dark)	2,700,000	2,800	88,000	11.9	27	42,000	3.5	5.2	2.9	1.2

standard samples (G-1, W-1, SY-1, BCR-1, AGV-1, GSP-1, G-2, PCC-1, and DTS-1) for calibration.

The spectrographic plates were examined to establish the presence or absence of all elements which have spectral lines in the wavelength regions covered (2450 to 4950 Å and 6100 to 8600 Å). Line interferences were checked for all lines. Several samples were brought from behind the biological barrier and analyzed by atomic absorption procedures. The data reported for these elements in sample 12013 were obtained by these methods. In all, 32 samples were processed, and a representative suite of 14 analyses is given in Table 2. Sample weights provided for analysis were typically from 100 to 150 mg.

The samples appear to be free from inorganic contamination, either from the rock box or from the lunar landing vehicle. Niobium, present at 88 percent in the skirt of the LM descent engine was detected in only two samples, 12013 with 170 ppm and 12033 with 44 ppm. This amount is almost certainly indigenous to the rocks, and its presence is consistent on geochemical grounds with the high abundance of associated elements Zr and Y. Indium, present in the seal of the rock boxes, was not detected. Sporadic copper contamination of up to several hundred parts per million was encountered.

Noble Gases

Several samples each of fine material, breccia, and crystalline rocks returned by Apollo 12 have been analyzed for noble gas isotopes. Analyses were performed by mass spectrometry, and the general technique used was the same as for the preliminary examination of Apollo 11 samples (*2*). As was the case for Apollo 11 material, the fines and breccia are characterized by large abundances of noble gases of solar wind origin, as exemplified by the large relative abundances of helium and by the characteristic ^{4}He/^{3}He and ^{20}Ne/^{22}Ne ratios. The crystalline rocks, on the other hand, contain much smaller amounts of noble gases which arise mainly from spallation reactions within the samples or from radiogenic decay. Table 3 lists noble gas isotopic contents for typical samples of all three types of lunar material from Apollo 12. Ratios are believed to be accurate to within ± 2 percent (except 4/3 which has a larger uncertainty) and abundances to within ± 20 percent (except ^{84}Kr, which is considerably greater).

In spite of the general similarity in noble gas content of Apollo 12 and the Apollo 11 material, there are several differences between the two. The noble gas contents of Apollo 12 fines and breccia are lower, the fines by a factor of 2 to 5 and the breccia by an order of magnitude. Using a model of formation of fine material by degradation of surface rock, surface irradiation by constant solar wind, and subsequent burial by additional fine material, the lower gas content of the fines implies a higher accumulation rate of material. The Apollo 12 breccias are approximately a factor of 2 lower in gas content than Apollo 12 fines. This constitutes a reversal of the trend observed with Apollo 11 material and implies that the Apollo 12 breccias were formed from fine material of lower solar wind gas content. Possibly the Apollo 12 breccias were formed at some distance or depth from their current lunar location.

For breccia 12034 the total noble gas content is low enough for a spallation component to be quite evident. Sample 12010 is an unusual case of a breccia-like rock which was identified on the basis of its noble gas content. It is characterized by a large relative abundance of lithic material, with dark gray, fine-grained material occurring as veins. In Table 1 the sample labeled "dark" 12010 contains about 70 percent of this fine-grained material, whereas that labeled "light" is essentially pure lithic material. The typical breccia-like nature of 12010 in terms of its noble gas content is obvious.

The ratio of ^{40}Ar to ^{36}Ar in Apollo 12 fines and breccia is lower than that for Apollo 11 (with the exception of 12010), although the ratio still shows larger values for breccia than for fines. Theoretical considerations prohibit 40/36 ratios even as large as 0.6 for the sun, making a solar wind origin of the ^{40}Ar unlikely. The amount of ^{40}Ar in the fines is too large to be generated by *in situ* decay of potassium; however, for the breccia this mode of origin may be possible. Excess ^{40}Ar of lunar origin thus appears to have been acquired by the fine material. The amount of ^{40}Ar and the 40/36 ratio in 12010 demonstrate this phenomenon. While the lithic phase resembles the other crystalline rock in its argon content, the fine-grained material shows not only large amounts of solar wind argon, but also large excesses of ^{40}Ar.

The crystalline rock samples reported here were completely interior chips and contain orders of magnitude less noble gas than does the fine material. The exceptions are ^{3}He, ^{21}Ne, ^{40}Ar, and some of the lighter isotopes of Kr and Xe, isotopes whose abundances have been greatly increased by spallation reactions and radioactive decay. Utilizing the potassium concentrations obtained for the rocks by the PET chemical analysis group, we have calculated K-Ar ages. Several crystalline rocks give ages between 1.7 and 2.7 $\times$ 10^9 years with an average value of 2.3 $\times$ 10^9. Rock 12013 has a unique chemistry, characterized in part by much higher abundances of K and U, and consequently also of radiogenic ^{4}He and ^{40}Ar. Our sample also contained excess radiogenic ^{40}Ar, rendering the K-Ar age meaningless. However, the U-Th-He age, as is the case for many of these crystalline rocks, is consistent with a value of about 2.3 $\times$ 10^9 years. This age is considerably below that found for the Apollo 11 crystalline rocks, although the range of ages for the two sites overlap. It appears that at least this portion of Oceanus Procellarum has a more recent crystallization age than the rocks sampled by Apollo 11 in Mare Tranquillitatis, which implies that lunar maria have a formation history of at least 1 billion years.

Cosmic-ray exposure ages, that is, integrated exposure time at the lunar surface, have been calculated for several rocks on the basis of 2π geometry and a ^{3}He production rate of 1 $\times$ 10^{-8} ccSTP/g-10^6 years. These ages show the much wider spread of 1 $\times$ 10^6 years from a piece of glass to 200 $\times$ 10^6 years with some apparent grouping of ages. The breccias also give radiation ages in this group. These exposure ages resemble those found for the Apollo 11 rocks. Spallation-produced isotopes other than ^{3}He are consistent with the ^{3}He ages and with the special chemistry of the lunar material. Because of the high alkaline earth, yttrium, and zirconium abundances, spallation-produced Kr and Xe are quite obvious in the rocks. The amounts of these gases are also roughly consistent with the chemistry.

Total Carbon Analyses

The total carbon content of the lunar samples was determined by oxygen combustion followed by gas chromatographic detection of CO_2 produced. Samples weighing 50 to 600 mg were placed together with iron chips and a copper-tin accelerator in a previously burned refractory crucible that was then heated in excess of 1600°C in a flowing oxygen atmosphere. The combustion products were analyzed with previously described procedures (*3*).

The system was calibrated with National Bureau of Standards, Steel Standard 101e. Samples of this standard, containing from 5 to 50 μg of carbon were analyzed under the same conditions as the lunar samples. In order to reduce the background the crucible was burned in air at 1000°C for at least 1 hour. Only crucibles heated to 1000°C in a single batch were utilized in a sequence of standards and samples. The precision of the method was evaluated by making replicate analyses on sample blanks. A typical standard deviation of a series of ten determinations was 2 μg of total carbon. The results for the standard samples were plotted on linear graph paper and the carbon content in lunar samples read directly from the standard linear curve.

Table 4. Total carbon analyses of Apollo 12 lunar samples.

Sample	Total carbon (ppm)
Fines	
12003	180
12024	115
12032	25
12033	23
12042	130
12059	200
Breccia	
12034	65
12057	120
Coarse-grained rocks	
12040	45
12044	44
Fine-grained rocks	
12052	34
12063	35
12065	31

The results of the analyses are given in Table 4. The highest carbon abundances, like those of Apollo 11 (*3*), tend to be found in the fines. Exceptions to this generalization are samples 12032 from the ejecta blanket of Bench crater and 12033 from the bottom of a trench at Head crater. The breccias are more abundant in carbon than the igneous rocks. The igneous rocks are consistently low in carbon. A total carbon abundance of about 40 ppm appears to be indigenous to lunar rocks. Additional carbon appears to have been added to the fines and subsequent breccias by meteoritic impact, solar wind, and possibly by contamination. The total carbon results alone give no indication of the specific chemical species present.

Gamma-Ray Spectrometry

Operation of the Radiation Counting Laboratory (RCL) followed the general procedures developed for Apollo 11 studies (*2*). The first RCL sample was received for measurement on 30 November 1969.

Analysis was performed by use of the NaI(TI) low-background spectrometer and on-line computer data acquisition system. Samples were mounted in stainless steel cans of 16.2-cm diameter and 0.8-mm wall thickness with bolt-type indium seals. Standard containers of overall heights of 5.6 or 7.6 cm were used for all rock samples. Fines were packages in a cylindrical container used in searches for magnetic monopoles.

Calibrations were obtained with a series of radioactive standards prepared by dispersing known amounts of radioactivity in quantities of iron powder. Time did not permit the recording of a library of standard spectra with the standard sources placed inside the steel containers actually used. Empirical corrections for the effects of the containers were applied; these corrections were least important for the ^{40}K data and most important for the ^{26}Al and ^{23}Na results.

The results are summarized in Table 5. Rather large errors have been assigned, which include the statistical errors of counting and estimates of possible systematic errors due to uncertainties in the detector efficiency calibration. The potassium concentration of the crystalline rocks is remarkably constant at about 0.05 weight percent, and the ratio K/U is about 2200. These properties are significantly lower than the typical crystalline rocks from Apollo 11; however, one of the coarsely crystalline Apollo 11 rocks (sample 10003) did resemble very closely the chemical composition of these crystalline rocks. The ratio of Th/U is about 4 for materials in Table 5, as found for the materials from Tranquillity Base. The concentrations of the radioactive elements K, Th, and U in the crystalline rocks are remarkably constant and on the average much lower than comparable Apollo 11 rocks. Because so few samples can be compared, it is possible that biased sampling of the lunar surface material is a factor in the differences between the soils and the rocks.

The breccia and fines are quite different from the crystalline rocks in several respects. The ratio K/U is only 1400 to 1500, compared with an average value of about 2800 for all Apollo 11 materials. Thus, these samples show even greater differences from terrestrial rocks and meteorites than did the surface material from Tranquillity Base. Although the ratio Th/U remains at about 4, the concentrations of all the radioactive elements are much higher in the breccias than in the crystalline rocks.

In general, the amount of cosmogenic ^{26}Al and ^{22}Na appear saturated, but show variations which may be related to chemical composition or to cosmic-ray exposure. For example, sample 12034, recovered from a trench dug during the lunar surface activities, was buried to a depth of 10 to 15 cm. The saturation activities of ^{26}Al and ^{22}Na are reduced by the approximate factor expected due to attenuation of the irradiation flux in the lunar soil.

Biology

To date no viable organism has been found in the lunar material and there is no evidence of previously living or fossil material.

Direct observations involved light microscopy utilizing white light, ultraviolet light and phase contrast techniques. A wide variety of biological systems are now undergoing tests with lunar material to determine if there is any toxicity, microbial replication, or pathogenicity. Germ-free in vivo systems include mice, plants, plant tissue cultures, and viral assay tissue cultures. Other in vivo tests on animals that are not germ-free include fish, insects, Japanese quail, oysters, flatworms, protozoans, and shrimp. Histological studies are being made to determine whether or not there is any evidence of pathogenicity. Other activities involve extensive in vitro study of the early biosample and of the regular lunar samples.

Organic Chemistry

A computer-coupled, high-sensitivity mass spectrometer has been used to estimate the abundances of organic matter in the lunar samples. Information on the volatile and pyrolyzable organic matter as a function of sample temperature has been obtained from detailed mass spectrometric data. From these data on the lunar samples as well as from blanks and controls, an assessment of the relative contributions of terrestrial contaminants as opposed to possible indigenous lunar organic matter has been made.

Samples were sealed in stainless steel vials with aluminum caps and heat sterilized at 130°C for 30 hours. Portions of these samples (35 to 500 mg) were transferred to a nickel container for mass spectral analysis. Samples representative of all rock types and core-tube fines were analyzed as well as appropriate blanks and controls. With the exception of the sample preparation protocol, the mass spectrometer–computer hardware and data acquisition, processing, and recording techniques were as described previously (*2*).

Table 5. Gamma-ray analyses of lunar samples.

Sample	Weight (g)	K (wt %)	Th (ppm)	U (ppm)	^{26}Al (dpm/kg)	^{22}Na (dpm/kg)	Other radionuclides detected	Remarks
12002	1530	0.044 ± 0.004	0.96 ± 0.1	0.24 ± 0.033	72 ± 14	53 ± 10	^{54}Mn, ^{52}Mn, ^{56}Co, ^{46}Sc, ^{48}V	Crystalline rock
12004	502	0.048 ± 0.004	0.88 ± 0.09	0.25 ± 0.033	112 ± 22	65 ± 13	^{54}Mn, ^{56}Co, ^{46}Sc, ^{48}V	Crystalline rock
12039	255	0.060 ± 0.005	1.20 ± 0.12	0.31 ± 0.040	80 ± 16	45 ± 9	^{56}Co, ^{54}Mn	Crystalline rock
12053	879	0.051 ± 0.004	0.89 ± 0.09	0.25 ± 0.033	85 ± 17	42 ± 9	^{56}Co, ^{48}V, ^{46}Sc, ^{54}Mn	Crystalline rock
12054	687	0.052 ± 0.004	0.77 ± 0.08	0.21 ± 0.030	50 ± 11	42 ± 9	^{48}V, ^{56}Co, ^{54}Mn, ^{46}Sc	Crystalline rock
12062	730	0.052 ± 0.004	0.81 ± 0.08	0.21 ± 0.030	65 ± 13	34 ± 7	^{48}V, ^{56}Co, ^{54}Mn, ^{46}Sc	Crystalline rock
12064	1205	0.053 ± 0.004	0.88 ± 0.09	0.24 ± 0.035	58 ± 12	44 ± 9	^{56}Co, ^{46}Sc, ^{48}V, ^{54}Mn	Crystalline rock
				Miscellaneous samples				
12034	154	0.44 ± 0.035	13.2 ± 1.3	3.4 ± 0.4	58 ± 12	27 ± 6	^{54}Mn	Breccia
12073	405	0.278 ± 0.022	8.2 ± 0.8	2.0 ± 0.3	125 ± 25	60 ± 12	^{56}Co, ^{54}Mn, ^{46}Sc	Breccia
12070	354	0.206 ± 0.016	6.0 ± 0.6	1.5 ± 0.2	140 ± 25	65 ± 13	^{56}Co, ^{48}V, ^{46}Sc, ^{54}Mn	Fines
12013	80	2.02 ± 0.016	34.3 ± 3.4	10.7 ± 1.6				Feldspathic differentiate

In comparison with the results reported from examination of Apollo 11 samples, the data obtained for the current samples as well as the controls indicate a significant reduction in the amount of Apollo Lunar Sample Return Container (ALSRC) and LRL organic contamination to values below the parts per million range. This situation has alleviated significantly the previous ambiguities in interpretation of data. The concentrations of organic material in the rock chips were between 0.1 and 0.4 ppm. The amounts for the fine material (gas analysis sample container, core tubes, and other fines) ranged from 0.3 to 1.0 ppm. A feature common to all the samples was the high yield of carbon dioxide. The evolution of CO_2 characteristically reaches a maximum rate at about 10 to 15 minutes after sample insertion into the mass spectrometer and then decreases, although in many cases it remains a significant contributor to the total ionization throughout the analysis (about 30 minutes). Mass spectra from the core-tube fines display ions up to the *m/e*-120 range which, if of aliphatic hydrocarbons, would be unsaturated, but not aromatic.

By comparison of the mass spectra and the volatilization characteristics of the evolved gases from the blanks and controls with the corresponding data on the lunar sample, most of the organic matter observed can be attributed to terrestrial contamination. The evolution of sulfur dioxide and relatively large quantities of carbon monoxide and carbon dioxide would be consistent with reactions of elemental carbon and sulfur with the mineral matrix.

A somewhat striking contrast is evident between the Apollo 11 and 12 material. There is no indication (based on the observations of *m/e*-78 and -91 late in the heating cycle) that pyrolysis of any indigenous organic matter is occurring in the Apollo 12 samples.

In conclusion, then, if there is any naturally occurring organic matter present in the Apollo 12 samples its concentration is extremely low, no more than 10 to 200 ppb.

Conclusions

The major findings of the preliminary examination of the lunar samples are as follows.

1) The conclusions reached concerning the rocks from Tranquillity base (*2*) also apply to the Apollo 12 rocks except as noted below.

2) Whereas all the Apollo 11 crystalline rocks displayed essentially one texture (lath-shaped ilmenite and plagioclase with interstitial pyroxene) and similar modes (50 percent pyroxene, 30 percent plagioclase, 20 percent opaque, 0 to 5 percent olivine), the Apollo 12 crystalline rocks show a wide range in both texture and mode.

3) Most of the igneous rocks fit a fractional crystallization sequence indicating that they represent either parts of a single intrusive sequence or samples of a number of similar sequences.

4) Breccias are of lower abundance at the Ocean of Storms site compared to Tranquillity Base presumably because the regolith at the Ocean of Storms is less mature and not as thick as at Tranquillity Base.

5) Complex stratification, presumably due mainly to the superposition of ejecta blankets, exists in the lunar regolith; a layer of volcanic ash may be present (sample 12033).

6) The greater carbon content of the breccias and fines compared to the crystalline rocks is presumably due largely to contributions of meteoritic material and solar wind.

7) The amount of indigenous organic material capable of volatilization or pyrolysis, or both, appears to be extremely low (that is, no greater than 10 to 200 ppb).

8) The content of noble gas of solar wind origin is less in the fines and breccias of the Apollo 12 rocks than in the fines and breccias from Tranquillity Base. The breccias contain less solar wind contribution than the fines, indicating that the breccias were formed from fines lower in solar wind noble gases than the fines presently at the surface.

9) The presence of nuclides produced by cosmic rays shows that the rocks have been within 1 m of the surface for 1×10^6 to 200×10^6 years.

10) The $^{40}K/^{40}Ar$ measurements on igneous rocks show that they crystallized 1.7×10^9 to 2.7×10^9 years ago.

11) The breccias and fines are similar chemically and contain only half the Ti content of the Apollo fines. The crystalline rocks contain less Ni, K, Rb, Zr, U, and Th than the fine material.

12) The Apollo 12 rocks contain less Ti, Zr, K, and Rb and more Fe, Mg, and Ni than the Apollo 11 samples.

13) Systematic variations among the Mg, Ni, and Cr contents occur in the crystalline rocks, but there are only small differences in the K and Rb contents.

14) Rock 12013 has a distinctive composition, similar to that of a late-stage basaltic differentiate. It contains higher amounts of Si, K, Rb, Pb, Zr, Y, Yb, U, Th, and Nb than previously encountered.

Discussion

Even though the preliminary examination has included only superficial scientific reconnaissance of samples which will be studied for years to come, a number of important findings have emerged, especially by comparison with the data for the Tranquillity Base rocks.

The chemistry of the two mare landing sites is clearly related and resembles Surveyor V and VI data. Both suites of rocks show the distinctive features of high concentrations of some refractory elements and low contents of volatile elements, which most clearly distinguish lunar from other materials. This overall similarity indicates that the sample composition of Apollo 11 material is not unique. It is clear that the geochemical problems raised by the Apollo 11 samples are still present in the Apollo 12 material.

Unlike the Tranquillity Base samples, the elemental abundances in the fines in the Apollo 12 samples display a generally more fractionated character than the rocks. The fine material and the breccias are generally quite similar in composition, and could not have formed directly from the large crystalline rock samples. The chemistry of the fine material is not uniform in the different maria.

The overall geochemical behavior of the rocks is consistent with the patterns observed during fractional crystallization in terrestrial igneous rocks involving olivine and pyroxene separation, depleting the silicate melt in elements such as Ni and Cr which preferentially enter these mineral phases, and enriching the residual melt in those elements such as Ba, K, and so forth excluded from the early crystal fractions. The slight degree of enrichment of the latter elements indicates an early stage of the fractional crystallization process. Sample 12038 fits neatly as a late stage in such a process. Whether these rocks form a related sequence or are a heterogeneous collection of similar origins cannot be answered from the chemical evidence.

The chemistry of the Apollo 12 samples is not identical with that of any known meteorite, nickel in particular being strikingly depleted. It has interesting similarities with the eucrites, however. Sample 12038 shows many similarities in composition. The concentration of Ti, Zr, Sr, and Ba are sufficient to distinguish them, but it now seems a fairly good possibility that rocks of similar chemistry to the eucritic meteorites are present on the moon, in view of the variation in composition observed between and at two maria sites. This possibility has previously been suggested (*4*). Even though these rocks are more similar to tholeiitic and alkaline basalts than the Apollo 11 rocks, there are still some striking dissimilarities.

The Apollo 12 material is enriched in many elements by one to two orders of magnitude in comparison with our estimates of cosmic abundances and the maria material is clearly strongly fractionated relative to our ideas of the composition of the primitive solar nebula.

The Apollo 12 site appears to be less geomorphologically mature than Tranquillity Base, with a thinner regolith. The lower amount of solar wind material in the fines, compared to those from Tranquillity Base, also suggests that Oceanus Procellarum mare material is younger than that in Mare Tranquillitatis.

The single most interesting scientific observations is the K-Ar age of the Apollo 12 rocks. The $^{40}K/^{40}Ar$ age of these rocks reinforces the probability that the lunar maria are geologically very old. If the minimum ages established by this method are indicative of the true age of the Apollo 12 rocks, then, compared with the Apollo 11 site, the mare material in Oceanus Procellarum at the Apollo 12 site is about 1 billion years younger. Although this K-Ar age is subject to various uncertainties, the younger age for the Apollo 12 material is consistent with geological observations. This large age difference indicates a prolonged period of mare filling.

References and Notes

1. The people who contributed directly to obtaining the data and to the preparation of this report are: D. H. Anderson, Manned Spacecraft Center (MSC); E. E. Anderson, Brown and Root-Northrop (BRN); Alan Bean, MSC; P. R. Bell, MSC; Klaus Biemann, Massachusetts Institute of Technology (M.I.T.); D. D. Bogard, MSC; Robin Brett, MSC; A. L. Burlingame, University of California at Berkeley; Patrick Butler, Jr., MSC; A. J. Calio, MSC; W. D. Carrier, MSC; E. C. T. Chao, United States Geological Survey (USGS); R. S. Clark, MSC; Charles Conrad, Jr., MSC; N. C. Costes, Marshall Space Flight Center; D. H. Dahlem, USGS; J. S. Eldridge, Oak Ridge National Laboratory (ORNL); M. S. Favaro, U.S. Public Health Service; D. A. Flory, MSC; C. D. Forbes, MSC; T. H. Foss, MSC; Clifford Frondel, Harvard University; R. Fryxell, Washington State University; John Funkhouser, State University of New York, Stony Brook; E. K. Gibson, Jr., MSC; E. N. Goddard, USGS; W. R. Greenwood, MSC; M. H. Hait, USGS; G. H. Heiken, MSC; R. S. Harmon, MSC; J. Hauser, University of California at Berkeley; Walter Hirsch, BRN; P. H. Johnson, BRN; J. E. Keith, MSC; C. F. Lewis, Arizona State University (ASU); John F. Lindsay, MSC; Gary E. Lofgren, MSC; V. A. McKay, ORNL; N. Mancuso, M.I.T.; J. D. Menzies, U.S. Department of Agriculture; J. K. Mitchell, University of California at Berkeley; Carleton B. Moore, ASU; D. A. Morrison, MSC; R. Murphy, M.I.T.; G. D. O'Kelley, ORNL; M. A. Reynolds, MSC; R. T. Roseberry, ORNL; G. C. Schaber, USGS; O. A. Schaeffer, State University of New York, Stony Brook; Ernest Schonfeld, MSC; J. W. Schopf, University of California at Los Angeles; R. F. Scott, California Institute of Technology; E. M. Shoemaker, California Institute of Technology; D. H. Smith, University of California at Berkeley; R. L. Smith, USGS; R. L. Sutton, USGS; G. A. Swan, USGS; S. R. Taylor, Australian National University; Jeff Warner, MSC; A. C. Waters, University of California, Santa Cruz; Ray E. Wilcox, USGS; D. R. Wones, M.I.T.; and J. Zahringer, Max-Planck-Institut, Heidelberg, Germany.
2. Lunar Sample Preliminary Examination Team, *Science* **165**, 1211 (1969).
3. C. B. Moore, C. F. Lewis, E. K. Gibson, Jr., W. Nichiporuk, *Science* **167**, 495 (1970).
4. M. B. Duke and L. T. Silver, *Geochim. Cosmochim. Acta* **31**, 1637 (1967).
5. The members of the LSPET wish to acknowledge the technical assistance of the Brown and Root-Northrup staff: John H. Allen, Travis J. Allen, A. Dean Bennett, L. E. Cornitius, J. B. Dorsey, Paul Gilmore, George M. Greene, William R. Hart, D. W. Hutchison, Robert W. Irvin, Carl E. Lee, J. D. Light, E. Allen Locke, J. Roger Martin, David R. Moore, Weldon B. Nance, Albert F. Noonan, David S. Pettus, Clifford M. Polo, W. R. Portenier, M. K. Robbins, Louis A. Simms, and R. B. Wilkin.

Doppler Shift Measurements of Nuclear Lifetimes

The concept of a Doppler shift is utilized in the measurement of lifetimes of nuclear excited states.

Jack R. MacDonald

The study of the excited states of nuclei represents a major area of interest in nuclear structure physics. By virtue of the motion of the protons and neutrons in the nucleus, either individually or collectively, most nuclei can exist in "excited" states with a prescribed (quantized) amount of energy in excess of that possessed by the nucleus in its "ground" state or state of lowest energy. In addition to its energy of excitation, a nuclear excited state can be characterized by its spin (angular momentum), its parity (spatial symmetry), and its decay properties, which include its lifetime and mode of decay. Each of these properties of nuclear excited states can be determined by appropriate experimental techniques. Of particular interest is the lifetime of the excited state, that is, the mean time a nucleus exists with a particular excess energy before it decays to a state of lower energy by the emission of one or more particles or the emission of gamma rays (relatively high-energy electromagnetic radiation). From a knowledge of nuclear lifetimes and other measurable properties of nuclear states, one attempts to deduce a model or theoretical description of the nucleus which may not only explain in a consistent fashion the observed properties of nuclei but may also lead to a greater understanding of the forces which hold nuclei together.

The measurement of nuclear lifetimes by use of a variety of experimental approaches has long been a study of considerable importance. One such technique, which utilizes the concept of a Doppler shift (*1*), was developed to a high degree of sophistication by Devons and others (*2*) in the early 1950's. This technique can, in principle, be applied to the measurement of lifetimes of a large and important class of nuclear states, namely, those which decay by gamma-ray emission. Until recently, however, these measurements were possible only in a relatively few cases. Recent technological advances have greatly facilitated lifetime measurements which utilize the principle of Doppler shifts to such an extent that the techniques are now routinely applied to the study of nuclear structure. In this article, I shall discuss the principle of the method and the experimental techniques and give some examples of experiments which have indeed furthered our knowledge of the structure of nuclei.

The Doppler Shift Principle

The measurement of time or of time intervals always involves the comparison of the unknown interval with a known time interval. For example, the age of a fossil can very often be determined by comparison with a known half-life of a radioactive isotope found in or near the fossil. Even more familiar is the measurement of time by comparison with a standard time interval produced by a mechanical or electrical device known as a clock. By sophisticated techniques, it is possible to measure intervals of time as short as a few tens of picoseconds (1 picosecond $= 10^{-12}$ second) with a form of electronic clock. However, many nuclear excited states have lifetimes much shorter than this, and it is in the region of 10^{-11} to 10^{-14} second that Doppler shift methods for the measurement of nuclear lifetimes have been of enormous importance.

The most familiar example of a Doppler shift is the change in pitch of a train whistle as the train moves toward and away from a listener. This difference in pitch or frequency of the sound waves depends upon the velocity of the train relative to the listener. It is this velocity-dependent change in frequency which is termed Doppler shift. The same concept applies to electromagnetic radiation emitted from a moving source—the frequency (and hence

---

The author is a Member of Technical Staff at Bell Telephone Laboratories, Incorporated, Murray Hill, New Jersey.